ARTICLE IN PRESS

Available online at www.sciencedirect.com

ScienceDirect

Ceramics International ▮ (▮▮▮▮) ▮▮▮–▮▮▮

CERAMICS INTERNATIONAL

www.elsevier.com/locate/ceramint

Origin of room temperature weak-ferromagnetism in antiferromagnetic $Pb(Fe_{2/3}W_{1/3})O_3$ ceramic

Shidaling Matteppanavar[a], Sudhindra Rayaprol[b], Anupama A.V.[c], Basavaraj Angadi[a,*], Balaram Sahoo[c]

[a]*Department of Physics, JB Campus, Bangalore University, Bangalore 560056, India*
[b]*UGC-DAE-Consortium for Scientific Research, Mumbai Centre, BARC Campus, Mumbai 400085, India*
[c]*Materials Research Centre, Indian Institute of Science, Bangalore 560012, India*

Received 12 May 2015; received in revised form 23 May 2015; accepted 23 May 2015

Abstract

We report the origin of room temperature weak ferromagnetic behavior of polycrystalline $Pb(Fe_{2/3}W_{1/3})O_3$ (PFW) powder. The structure and magnetic properties of the ceramic powder prepared by a Columbite method were characterized by X-ray and neutron diffraction, Mössbauer spectroscopy and magnetization measurements. Rietveld analysis of diffraction data confirm the formation of single phase PFW, without traces of any parasitic pyrochlore phase. PFW was found to crystallize in the cubic structure at room temperature. The Rietveld refinement of neutron diffraction data measured at room temperature confirmed the G-type antiferromagnetic structure of PFW in our sample. However, along with the antiferromagnetic (AFM) ordering of the Fe spins, we have observed the existence of weak ferromagnetism at room temperature through: (i) a clear opening of hysteresis (*M–H*) loop, (ii) bifurcation of the field cooled and zero-field cooled susceptibility; supported by Mössbauer spectroscopy results. The *P–E* loop measurements showed a non-linear slim hysteresis loop at room temperature due to the electronic conduction through the local inhomogeneities in the PFW crystallites and the inter-particle regions. By corroborating all the magnetic measurements, especially the spin glass nature of the sample, with the conduction behavior of the sample, we report here that the observed ferromagnetism originates at these local inhomogeneous regions in the sample, where the Fe-spins are not perfectly aligned antiferromagnetically due to the compositional disordering.

Keywords: Columbite method; Neutron diffraction; Compositional disorder; Weak ferromagnetism

1. Introduction

Magnetoelectric (M-E) – multiferroic materials possessing both ferroelectric and magnetic properties together in a single-phase compound are of tremendous interest not only for practical applications but also for fundamental understanding of the underlying physics of spintronic materials [1–4]. The intrinsic property of these materials is that they couple the electric polarization with the magnetization which allows an additional degree of freedom in the design of conventional multifunctional devices [5,6]. A range of new materials and device applications are possible taking advantage of these unique material characteristics [1–8]. Materials showing multiferroic properties at room temperature have additional advantage since they are the most preferred materials for device applications. Among all the (near-) room temperature multiferroic compounds discovered so far, $Pb(Fe_{2/3}W_{1/3})O_3$ (PFW) has the unique properties of having a high degree of order parameter and practically viable magnetic (paramagnetic-to-antiferromagnetic) ordering at T_N ~350–380 K; with paraelectric to ferroelectric phase transition temperature (T_C) ~150–200 K [9]. Recently, M–E coupling between the ferroelectric and antiferromagnetic orders in PFW (and related materials) was observed through an anomaly in the lattice parameters variation [9], variation of dielectric constant at T_N [10] and through a change in the dielectric constant induced by an external magnetic field [10].

*Corresponding author. Tel.: +91 80 2296 1478; fax: +91 80 2321 9295.
E-mail address: brangadi@gmail.com (B. Angadi).

http://dx.doi.org/10.1016/j.ceramint.2015.05.131
0272-8842/

Please cite this article as: S. Matteppanavar, et al., Origin of room temperature weak-ferromagnetism in antiferromagnetic $Pb(Fe_{2/3}W_{1/3})O_3$ ceramic, Ceramics International (2015), http://dx.doi.org/10.1016/j.ceramint.2015.05.131

In spite of these above qualities, limited progress has been made in the applications of PFW during the last several decades due to the following inherent limitations. The synthesis of single phase PFW with perovskite phase had been very difficult through the conventional solid-state reaction methods due to the formation of unwanted phases (for example $PbWO_4$ and $Pb_2W_2O_7$ pyrochlore). M–E coupling in known single-phase compounds is too weak to be used for practical applications and there were only a few compounds ($TbMnO_3$ and RMn_2O_5 (R = Tb, Dy, Ho)) exhibiting magnetoelectric coupling. The ferroelectric and magnetic property of PFW has been already the focus of a number of earlier studies [4,9–12]. For M–E device applications the existence of ferromagnetism is more desirable than antiferromagnetism. Imposing the desired ferromagnetism (along with the existing antiferromagnetic structure of PFW) at the ferroelectric transition temperature (< 200 K) remains a challenge. Fraygola et al. [13], Ye et al. [4] and Ivanov et al. [9] have observed weak ferromagnetic behavior in their PFW ceramic without clearly discussing about its origin in detail.

In this work, we have synthesized single-phase PFW ceramic powder by the Columbite method and characterized its room temperature crystal and antiferromagnetic structure using neutron diffraction (ND). To assess the weak ferromagnetism at room temperature, we have performed magnetization measurements, Mössbauer spectroscopy and polarization (*P–E* loop) measurements for the PFW ceramic at room temperature. Furthermore, we report the origin of this weak ferromagnetic behavior at room temperature in PFW.

2. Experimental details

PFW has been prepared by the Columbite (solid-state reaction) method [11] using high-purity (~99.9%) starting materials: PbO (SD Fine Chem. Lab.), Fe_2O_3 (Fluka) and WO_3 (SD Fine Chem. Lab.). Detailed synthesis method of PFW is reported elsewhere [12]. In brief, Fe_2O_3 and WO_3 were taken in stoichiometric quantities and ground in agate pestle and mortar in ethanol medium for ~2 h. The dried Fe_2WO_6 (Columbite) powder was calcined at 1000 °C for 4 h. After calcination, the Fe_2WO_6 powder was ground again and mixed in stoichiometric quantity with PbO and calcined at 900 °C for 2 h. After this second calcination stage, the obtained PFW powder was ground again by adding polyvinyl alcohol (PVA). Pellets of 10 mm (or, 5 mm) in diameter and 2–3 mm thickness were uniaxially cold pressed using 50 kN pressure using a hydraulic press. The pellets were sintered at 850 °C for 90 min in a closed Pb rich environment to minimize the PbO evaporation.

The sintered ceramic powder were characterized by X-ray diffraction (XRD; Phillips 1070) using Cu-Kα radiation (wavelength, $\lambda = 1.5406$ Å), to obtain the crystal structure. Fig. 1(a) shows XRD pattern of the PFW ceramic sample. Neutron diffraction measurements (Fig. 1(b)) were carried out on a focusing crystal based powder diffractometer, available at UGC-DAE-CSR beam line in Dhruva reactor, BARC. Neutrons at wavelength 1.48 Å were used for the present study.

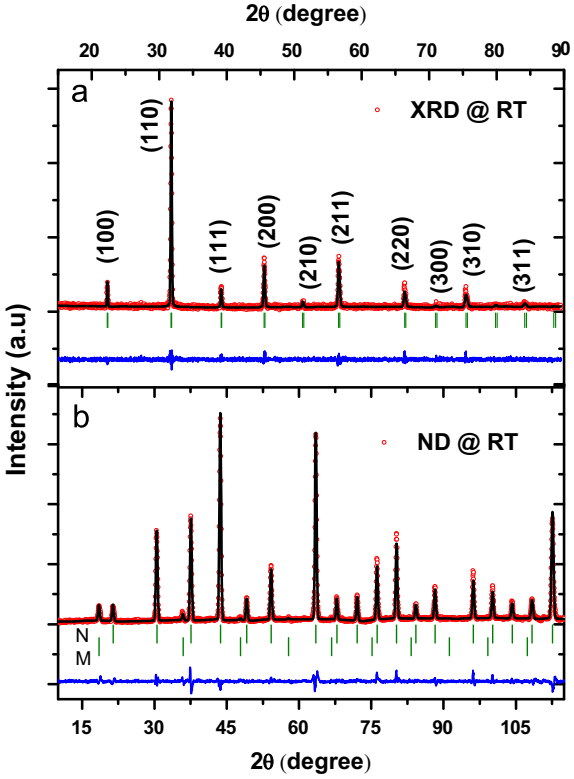

Fig. 1. (a) X-Ray diffraction pattern and (b) neutron diffraction pattern of sintered $Pb(Fe_{2/3}W_{1/3})O_3$ sample. The observed data points are shown by (red) circles, whereas the continuous lines passing through the data points is the calculated profile. The (blue) line at the bottom of the figure indicates the difference between observed and calculated profiles. Bragg positions are marked by the vertical (green) lines. In (b), first row marked with 'N' represents nuclear (crystallographic) Bragg peak positions and the second row marked with 'M' represents magnetic Bragg peak positions. (For interpretation of the references to color in this figure legend, the reader is referred to the web version of this article.)

Rietveld analysis were carried out on powder XRD and ND data using the Fullprof suite programs for crystallographic as well as for magnetic structure studies [14]. The obtained crystallographic and magnetic structures are shown in Fig. 2(a) and (b).

Magnetization studies were carried out on a vibrating sample magnetometer (VSM) attached to a physical property measurement system (Quantum Design PPMS). Fig. 3 shows the *M–H* loop of our PFW sample measured at room temperature up to an applied field of 90 kOe. Fig. 4 shows the zero field cooled (ZFC) and field cooled (FC) variation of magnetic susceptibility ($\chi = M/H$) with temperature for the PFW sample, measured in a field of 500 Oe.

^{57}Fe Mössbauer spectroscopy is one of the most efficient tools to investigate the local magnetic ordering, behavior and oxidation state of the iron atoms in the matrix. Transmission Mössbauer spectrum was measured at room temperature by using a ^{57}Co source (Rh – matrix, ~15 mCi) mounted on a constant acceleration Mössbauer drive from SEE Co., USA and a proportional counter. The room temperature Mössbauer spectrum for PFW sample is shown in Fig. 5. The spectrum is a Zeeman split six line pattern, where the black dots represent

Please cite this article as: S. Matteppanavar, et al., Origin of room temperature weak-ferromagnetism in antiferromagnetic $Pb(Fe_{2/3}W_{1/3})O_3$ ceramic, Ceramics International (2015), http://dx.doi.org/10.1016/j.ceramint.2015.05.131

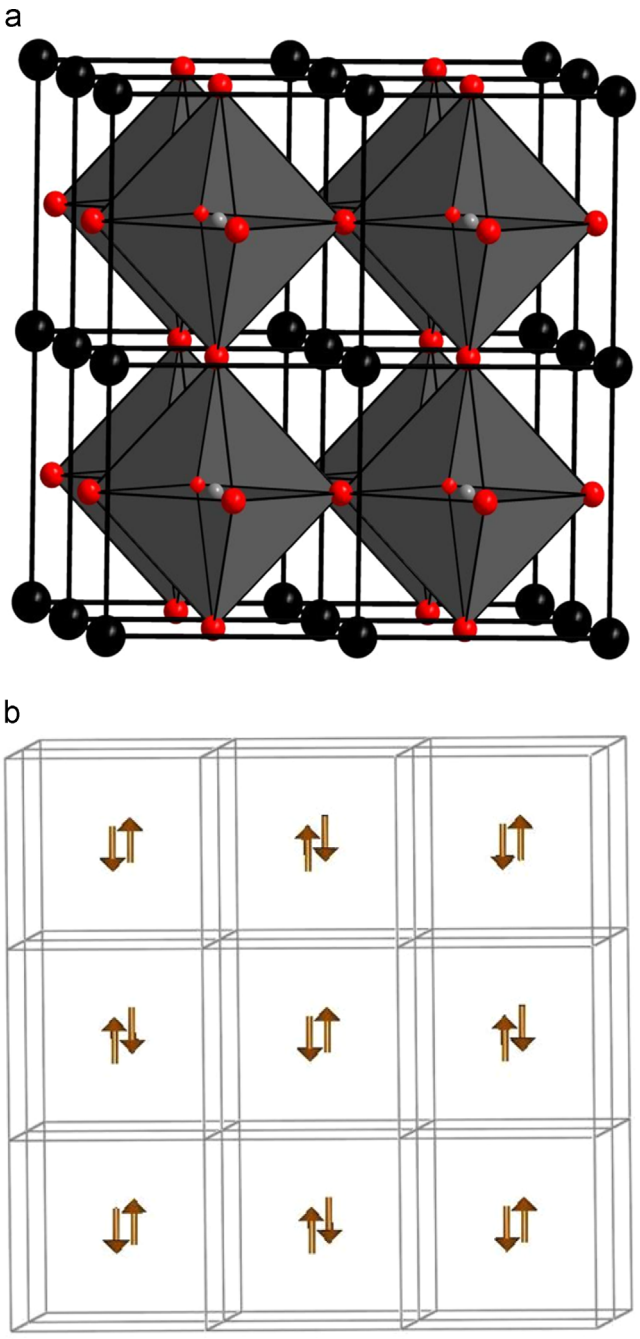

Fig. 2. (a) Crystal structure of $Pb(Fe_{2/3}W_{1/3})O_3$. The lead atoms are located at the edges of the unit cell. Polyhedron is drawn around the iron / tungsten atoms. Oxygen atoms are shown in red (at the edges of the polyhedra). (b) Magnetic structure of $Pb(Fe_{2/3}W_{1/3})O_3$. Only the moment on iron is shown as arrows. The alternative arrangement of arrows indicates the antiferromagnetic arrangement of magnetic ions, giving rise to the antiferromagnetic ordering at room temperature in PFW. (For interpretation of the references to color in this figure legend, the reader is referred to the web version of this article.)

the experimentally recorded data points and the solid line is the least square fit to the measured data. The spectrum recording time was about one week, but still the signal/noise ratio of the spectrum is low due to the electronic absorption of Pb and W. For the least – squares fitting of the Mössbauer spectrum we used the computer program *NORMOS* written by Brand [15].

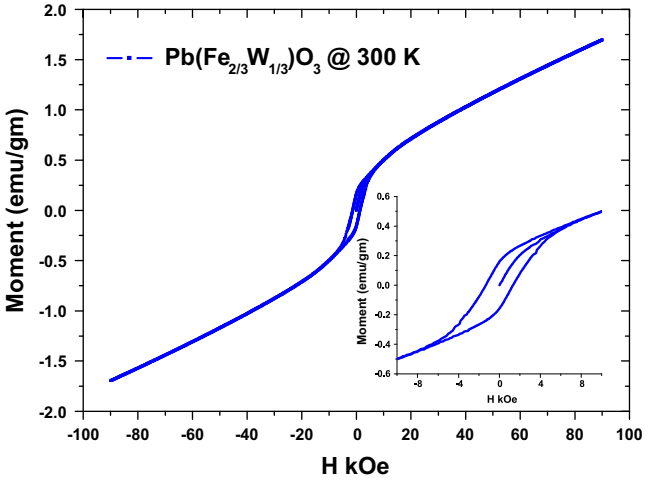

Fig. 3. Magnetization of $Pb(Fe_{2/3}W_{1/3})O_3$ measured as a function of varying magnetic field at 300 K. Inset shows the enlargement (around the origin) view for clarity.

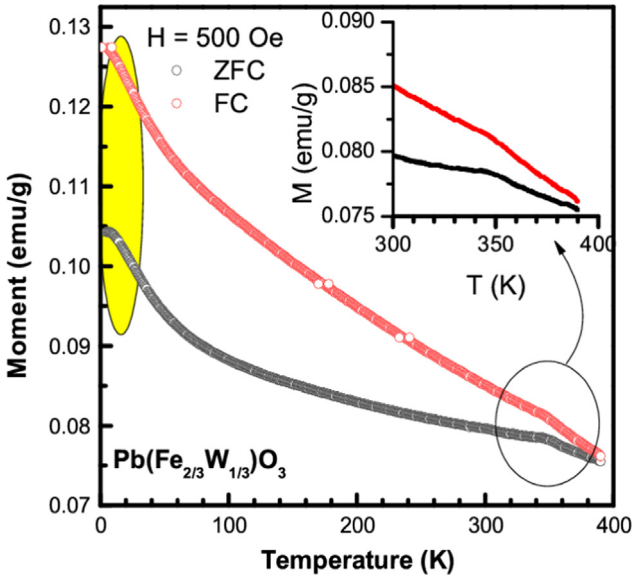

Fig. 4. Temperature dependent molar susceptibility (ZFC and FC) for $Pb(Fe_{2/3}W_{1/3})O_3$ at 500 Oe. Inset shows the molar susceptibility around the antiferromagnetic transition temperature $T_N \approx 350$ K. Shaded region shows the 2nd magnetic phase transition (blocking temperature) for the spin-glass behavior.

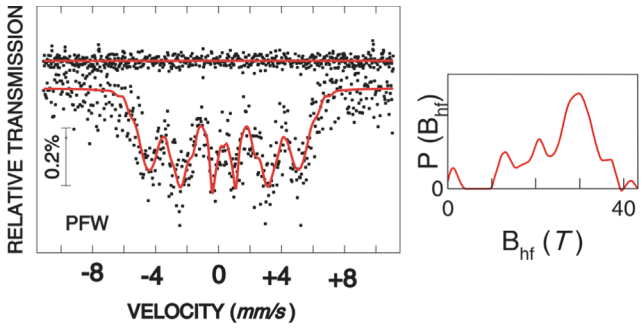

Fig. 5. Room temperature Mössbauer spectrum of $Pb(Fe_{2/3}W_{1/3})O_3$ sample. The figure at the right hand side shows the hyperfine field distribution, $P(B_{hf})$.

Please cite this article as: S. Matteppanavar, et al., Origin of room temperature weak-ferromagnetism in antiferromagnetic $Pb(Fe_{2/3}W_{1/3})O_3$ ceramic, Ceramics International (2015), http://dx.doi.org/10.1016/j.ceramint.2015.05.131

The ferroelectric (*P–E*) loop measurements were carried out at room temperature by ferroelectric loop (*P–E*) tracer (M/s Radiant Instruments, USA). Thin silver paste is applied on both sides (top and bottom) of the PFW ceramic pellet as the electrodes. For room temperature, *P–E* measurements, the samples were immersed in silicone oil to prevent the electric arcing, if any, at high applied voltages.

3. Results and discussion

3.1. Crystal structure: XRD and ND

The structural parameters for the prepared sample were obtained from the Rietveld refinement of the XRD data (Fig. 1(a)). The analysis confirms that the sample forms in single phase cubic structure (*Pm-3m* space group), with no secondary parasitic phases like $PbWO_4$ or $Pb_2W_2O_7$ etc. [12]. This suggests that the low temperature calcination and sintering proved to be effective in achieving the single phase without any impurity phases. Good agreement was found between observed and calculated profiles for XRD data.

Fig. 1(b) shows Rietveld refined room temperature ND pattern, which further confirms the cubic structure (*Pm-3m* space group) of the PFW sample. While refining for the crystallographic (nuclear) structure, thermal parameters and occupancies were also refined along with the cell parameters to obtain a reasonable agreement between observed and the calculated profiles. The structural model used in refining the powder XRD data was taken as starting model for the refinement of the ND data. The refined cell parameter from the analysis of room temperature ND data is $a=3.9776(4)$ Å, which is in good agreement with the XRD result ($a=3.9812$ (4) Å). The obtained *R*-factors ($R_p=4.87$ %; $R_{wp}=6.72$ %; $R_{exp}=2.84$ %; $\chi^2=5.60$, Bragg *R*-factor=3.65, *Rf*-factor=2.25) are also found to be reasonably good [9]. The structure of PFW can be described as follows: the lead ion is placed at the origin of the cell, at Wyckoff position, 1*a* i.e., (0, 0, 0). The transition metal ions, Fe and W are distributed randomly on crystallographic position given by the Wyckoff notation, 1*b,* i.e., (½, ½, ½), which is placed half-cell apart from Pb. Oxygen is placed between Pb and Fe/W, and forms a common face between Pb and Fe/W at Wyckoff site, 3*c* i.e., (½, ½, 0). Fig. 2(a) shows the crystallographic structure of PFW drawn based on the refinement results of room temperature ND data.

The room temperature ND pattern (Fig. 1(b)) clearly shows extra Bragg peaks around 2θ (or Q^{-1}) of 18.52° (1.36 $Å^{-1}$); 35.89° (2.61 $Å^{-1}$) and 47.77° (3.43 $Å^{-1}$). All these peaks could be identified as magnetic peaks and were indexed using a single propagation vector $k=(½, ½, ½)$. For refinement, symmetry elements and basis vectors of the irreducible representations were obtained using *BasIreps* program within the Fullprof suite [16]. The magnetic phase was added as the second phase, and the refinement was carried out assuming Fe as the only magnetic ion in PFW. A successful magnetic structure obtained was a G-type antiferromagnetic structure. The value of the magnetic moment per Fe ion at 295 K is 5.5 μ_B which is slightly lower than the calculated spin only value of 5.9 μ_B per Fe. The obtained *R*-factor for the magnetic phase (magnetic *R*-factor) is 23.0.

Fig. 2(b) shows the arrangement of magnetic moment (spins) in the magnetic structure of PFW as obtained from the Rietveld refinement of the ND pattern. The Fe^{3+} moments are arranged in a simple G-type structure as shown by arrows in Fig. 2(b). One Fe^{3+} spin is surrounded by six anti-parallel spins on the nearest neighbor Fe^{3+} ions.

3.2. Magnetization studies

PFW is a G-type antiferromagnetic material, whose magnetization behavior has been widely studied [4,9]. From the *M–H* loop of our PFW sample in Fig. 3, it can be observed that the magnetization displays a small hysteresis only in the low-field region. The appreciable opening of the hysteresis loop reveals the presence of weak ferromagnetism in our sample with a coercive field (H_c) value of 1.34 kOe. The inset in Fig. 3 shows the zoomed in view of the *M–H* loop around the origin for clarity. The saturated magnetization (M_s) and remnant magnetization (M_r) were estimated to be 0.24 emu/g and 0.16 emu/g, respectively. For higher applied magnetic fields, the magnetization increases linearly. This paramagnetic-like linear increase of the magnetization at the high field region can be assigned to the weakening of the super-exchange interaction of Fe^{3+}–O–W–O–Fe^{3+}, caused by the local disorder/short-range order of the Fe atoms at the B site.

The ZFC curve in Fig. 4 shows that χ increases monotonically on decreasing temperature from 400 K to ~350 K; and it exhibits a clear cusp around 350 K (T_{N1}) before increasing further down to a temperature of ~5 K. The cusp at ~350 K corresponds to the paramagnetic (PM) to antiferromagnetic (AFM) phase transition. This agrees well with reported T_N value of 340–380 K [9]. This lower value of the T_N can be attributed to the fluctuations in the local ordering of Fe and W ions. The increase in the value of χ starting from 400 K down to 5 K can be attributed to a modified-exchange interaction of Fe^{3+}–O–Fe^{3+} in the disordered regions of the PFW sample. Furthermore, the formation of the disordered regions might be due to the synthesis methods adopted, where the grain growth occurs with lattice strain/stress in the material which affects the T_N. However, it can be noticed that χ exhibits another cusp around 10 K (T_{N2}) before falling rapidly as temperature approaches 5 K. Our susceptibility data are in good agreement with the earlier reported results [4,9].

This magnetic anomaly at lower temperatures (around T_{N2}, 10 K) and the pronounced splitting in ZFC and FC curves observed below 380 K can be understood by considering the existing spin glass nature in the sample due to the compositional disorder. This can also be the origin of weak ferromagnetic ordering in the PFW ceramic. In our recent work [17] and the work by Chillal et al. [18], it is reported that for $Pb(Fe_{1/2}Nb_{1/2})O_3$ (a similar system like the present system (PFW)), two types of magnetic order emerge independently: (i) infinite-range percolation cluster (antiferromagnetic order) and (ii) (Fe^{3+} ions unblocked) super-antiferromagnetic Fe^{3+}

Please cite this article as: S. Matteppanavar, et al., Origin of room temperature weak-ferromagnetism in antiferromagnetic $Pb(Fe_{2/3}W_{1/3})O_3$ ceramic, Ceramics International (2015), http://dx.doi.org/10.1016/j.ceramint.2015.05.131

clusters. The coexistence of both of the above systems leads to a single homogenous phase, with the magnetic moments arranged in a speromagnetic-like or spin-glass-like fashion. We expect a similar magnetic ordering is present in our PFW sample too. This speromagnetic-like behavior is responsible for the existing weak ferromagnetic ordering at room temperature in our sample. Furthermore, the decrease in χ in the ZFC curves could be a result of the super-antiferromagnetic blocking of the local super-paramagnetic-like clusters present in the sample, confirming the presence of magnetic clusters in the sample having spin glass nature.

One may expect a magnetic anomaly at $\sim$150 K, the ferroelectric ordering temperature (T_C) of PFW. However, we have not observed any anomaly in magnetization. Furthermore, the bifurcation in ZFC and FC curves seen in the entire temperature range of measurement (Fig. 4) indicates presence of some ferromagnetic interactions in this system well above T_N and T_C. Hence, both the types of magnetic ordering (antiferromagnetic and spin-glass like) might be therefore taking place independently of the ferroelectric ordering in PFW. The Mössbauer results (see Section 3.3) further supports the presence of these two types of magnetic clustering due to compositional disorder. This kind of magnetic interaction is common in complex structured lead based systems, where the B site is occupied by a magnetic and a non-magnetic cation. According to earlier reports, compounds with good compositional ordering, such as $Pb(Co_{1/2}W_{1/2})O_3$, shows a single magnetic ordering temperature (T_N) at 8 K [19]. However, for $Pb(Fe_{1/2}Nb_{1/2})O_3$ [20,21] and $Pb(Fe_{1/2}Ta_{1/2})O_3$ [20,22,23], where a complete compositional ordering could not be achieved, showed two magnetic phase transition temperatures (T_{N1} $\sim$161 K and T_{N2} $\sim$9 K for $Pb(Fe_{1/2}Nb_{1/2})O_3$ and, T_{N1} $\sim$143 K and T_{N2} $\sim$9 K for $Pb(Fe_{1/2}Ta_{1/2})O_3$), suggesting the presence of disordered and ordered nanostructure.

3.3. Mössbauer spectroscopic studies

The Mössbauer spectrum (Fig. 5) of the PFW sample measured at room temperature was fit with a distribution of magnetic hyperfine fields, $P(B_{hf})$. The hyperfine field distribution is shown in the right hand side of Fig. 5. The obtained average isomer shift (IS) of 0.336 ± 0.005 mm/s, quadruple splitting (QS) of -0.017 ± 0.005 mm/s, corresponds to the Fe^{3+} ions in an octahedral environment [24]. The average magnetic hyperfine field is $\sim 25.5 \pm 1.0$ T. The broad hyperfine field distribution, $P(B_{hf})$ indicates that the environments of the Fe-ions are not the same, i.e., perfect compositional ordering is not achieved in the studied sample.

$P(B_{hf})$ for our sample is very similar to that of the earlier report by Raevskii et al. [24], where they fit the spectrum with a superposition of two sextets and a central (paramagnetic) doublet. From the $P(B_{hf})$ of our sample it is also clear that along with the broad magnetic hyperfine field distribution, there exists a paramagnetic part (the peak close to 2 T in $P(B_{hf})$, Fig. 5). Previously, Venevtsev et al. [25] reported a similar spectrum consisting of two sextets observed after firing the PFW ceramics in oxygen, while the spectrum consists of a single sextet for a sample fired in air. The existence of a single sextet was due to fully disordered arrangement of Fe^{3+} ions, while the two sextets in a Mössbauer spectrum for PFW was associated with a partial disordering of Fe^{3+} and W^{6+} ions. The formation of two magnetic subsystems might be due to non- equivalent surrounding of iron ions in partially ordered and disordered regions. According to calculations by the Guillaud method [26,27], the values of T_N for PFW for the order parameters $S \approx 1$ and $S \approx 0$, were 310 K and 460 K, respectively. S=1 and S=0 corresponds to the perfectly ordered and perfectly disordered state, respectively. The values of $T_N \approx 355$ K and $T_N \approx 425$ K were obtained experimentally for PFW ceramics synthesized and sintered in oxygen atmosphere, respectively, but, for samples sintered in air a T_N of 363 K was obtained [25,27].

We too believe that, there is partial disordering in our sample which gives rise to the broad hyperfine field distribution, $P(B_{hf})$. Despite the fact that our measurements were made at a temperature approximately 50 K below T_N (350 K, Fig. 4), the Mossbauer spectrum for PFW contains a paramagnetic component (the peak close to 2 T in $P(B_{hf})$). This component might be associated with such clusters in the sample where the degree of ordering is higher than the volume average. The observed results confirm that there are regions where the Fe atoms are compositionally disordered. This disordering breaks the antiferromagnetic ordering of PFW and shows the room temperature weak ferromagnetism as observed in the magnetization studies (Section 3.2).

3.4. Ferroelectric studies

The P–E hysteresis loop for the PFW measured in a field of ± 4 kV/cm is shown in Fig. 6. The loop shows no proper saturation polarization (P_S) with the applied external electric field. At room temperature (well above the Curie temperature (T_C=150 K) of PFW), the non-linear slim hysteresis is clearly an indication that the loop originates due to the leakage current in the sample. Furthermore, this leakage current confirms the

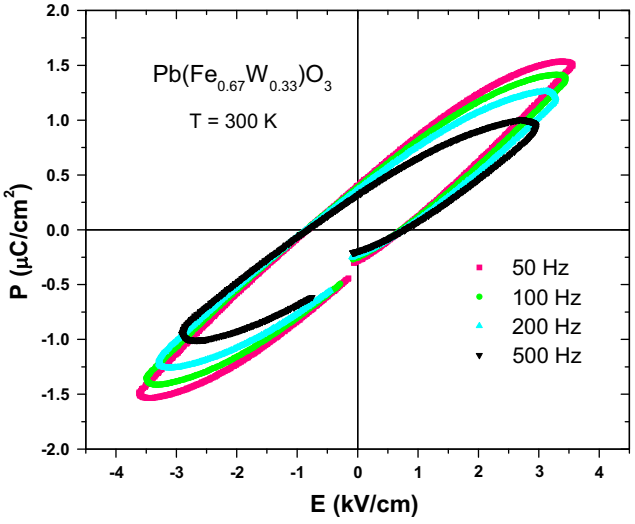

Fig. 6. Room temperature P–E loops measured at different frequencies.

Please cite this article as: S. Matteppanavar, et al., Origin of room temperature weak-ferromagnetism in antiferromagnetic $Pb(Fe_{2/3}W_{1/3})O_3$ ceramic, Ceramics International (2015), http://dx.doi.org/10.1016/j.ceramint.2015.05.131

presence of defected-, non-stoichiometric- or disordered-regions in the sample, which forbids application of high voltage.

It is worth noting that in ND we have not observed any ferromagnetic ordering of the magnetic moments. But, we have observed clear M-H (hysteresis) loop (Section3.2) justifying the presence of ferromagnetism. Hence, from the leakage current based-*P-E* loops, it is clear that the weak ferromagnetism observed in *M–H* loop of the antiferromagnetic PFW sample, at room temperature, originates from the defected-, non-stoichiometric- or disordered-regions and is isolated from the perfect antiferromagnetism of the PFW sample.

4. Conclusions

PFW ceramic were successfully synthesized by the Columbite method at relatively low calcination and sintering temperatures, following the closed environment sintering technique. Rietveld refinement of the room temperature XRD and ND results showed that the PFW sample was single-phased with cubic perovskite structure (*Pm-3m* space group), without any traces of pyrochlore phases. The magnetic structure of PFW refined using room temperature ND data, revealed the presence of G-type antiferromagnetic structure. The ND and Mössbauer spectroscopy results confirmed the Fe^{3+} (high spin) state of the Fe ions. It further suggested that the iron and tungsten atoms are randomly distributed at the available octahedral sites indicating the existence of compositional disorder. The temperature dependent magnetic susceptibility (χ vs. T) of PFW exhibited two inflexion points: one at $\sim$350 K corresponding to the Néel temperature (T_{N1}) and another at $\sim$10 K (T_{N2}) corresponding to a spin-glass like transition. The room temperature weak ferromagnetism, spin glass type FC–ZFC curve and anti-ferromagnetic ordering at $\sim$350 K suggests that the anti-ferromagnetism and the ferromagnetism originate from different regions in the sample.

Although, the antiferromagnetic ordering has been observed by temperature-dependent ND measurements [9], no signatures of long range ferromagnetic ordering were observed in ND data analysis. This suggests that the antiferromagnetism in this sample is long-ranged, but the weak ferromagnetism originate from the local uncompensated spins of the compositionally disorder Fe atoms in PFW sample. The χ vs. T measurement corroborates the above results confirming the fact that the existence of weak ferromagnetism is due to the super-paramagnetic/spin-glass-like behavior of the PFW sample at room temperature.

PFW has ferroelectric and antiferromagnetic transition temperatures of $\sim$150 K [9] and $\sim$350 K, respectively. The observed *P–E* loops measured at room temperature are believed to be originated due to the leakage current in the sample. The observed leakage current is due to the conduction through the local defects/inhomogeneities in the PFW crystallites and the inter-particle regions. Hence, the local compositionally disordered regions are responsible for the origin of weak ferromagnetism in PFW at room temperature.

Acknowledgments

SM and BA are thankful to the UGC-DAE-CSR, Mumbai centre for the financial support and experimental facilities, through the Collaborative Research Project Number CRS-M-159. Authors are thankful to Dr. V. R. Reddy and Sanjay Kumar Upadhyay, UGC DAE CSR Indore, for providing *P–E* loop measurement facility.

References

[1] N.A. Spaldin, M. Fiebig, The renaissance of magnetoelectric multiferroics, Science 309 (2005) 391–392.
[2] W. Prellier, M.P. Singh, P. Murugavel, The single-phase multiferroic oxides: from bulk to thin film, J. Phys.: Condens. Matter 17 (2005) R803–R832.
[3] M. Fiebig, Revival of the magnetoelectric effect, J. Phys. D: Appl. Phys. 38 (2005) R123–R152.
[4] Z.G. Ye, K. Toda, M. Sato, Synthesis, structure and properties of the magnetic relaxor ferroelectric $Pb(Fe_{2/3}W_{1/3})O_3$ [PFW], J. Korean Phys. Soc. 32 (1998) S1028–S1031.
[5] M. Fiebig, T.h. Lottermoser, D. Frohlich, A.V. Goltsev, R.V. Pisarev, Observation of coupled magnetic and electric domains, Nature 419 (2002) 818–820.
[6] T. Kimura, T. Goto, K. Thizaka, T. Arima, Y. Tokura, Magnetic control of ferroelectric polarization, Nature 426 (2003) 55–58.
[7] N. Hur, S. Park, P.A. Sharma, J.S. Ahn, S. Guha, S.W. Cheong, Electric polarization reversal and memory in a multiferroic material induced by magnetic fields, Nature 429 (2004) 392–395.
[8] T. Lottermoser, T. Lonkai, U. Amann, D. Hohlwein, J. Ihringer, M. Fiebig, Magnetic phase control by an electric field, Nature 430 (2004) 541–544.
[9] S.A. Ivanova, S.-G. Eriksson, R. Tellgren, H. Rundlof, Neutron powder diffraction study of the magnetoelectric relaxor $Pb(Fe_{2/3}W_{1/3})O_3$, Mater. Res. Bull. 39 (2004) 2317–2328.
[10] J.T. Wang, C. Zhang, Z.X. Shen, Y. Feng, Magnetic field effect on dielectric properties of $Pb(Fe_{1/2}Nb_{1/2})O_3$ single crystal, Ceram. Int. 30 (2004) 1627–1630.
[11] V.V. Bhat, B. Angadi, A.M. Umarji, Synthesis, low temperature sintering and property enhancement of PMN–PT ceramics based on the dilatometric studies, Mater. Sci. Eng. B 116 (2005) 131–139.
[12] S. Matteppanavar, B. Angadi, S. Rayaprol, Neutron diffraction studies on chemical and magnetic structure of multiferroic $PbFe_{0.67}W_{0.33}O_3$, AIP Conf. Proc. 1591 (2014) 1669–1671.
[13] B. Fraygola, A. Mesquita, A.A. Coelho, D. Garcia, V.R. Mastelaro, J.A. Eiras, Fe valence fluctuations andmagnetoelastic coupling inPb-based multiferroics perovskites, Phys. Status Solidi (A) 210 (2) (2013) 386–390.
[14] J. Rodriguez-Carvajal, Recent advances in magnetic structure determination by neutron powder diffraction, Physica B 192 (1993) 55–69.
[15] R.A. Brand, Nucl. Instrum. Methods B 28 (1987) 398.
[16] J. Rodriguez-Carvajal, BASIREPS: a program for calculating irreducible representations of space groups and basis functions for axial and polar vector properties, Solid State Phenom. 170 (2011) (2007) 263.
[17] S. Matteppanavar, S. Rayaprol, A.V. Anupama, B. Sahoo, B. Angadi, On the room temperature ferromagnetic and ferroelectric properties of $Pb(Fe_{1/2}Nb_{1/2})O_3$, J. Supercond. Nov. Magn. (2015) http://dx.doi.org/10.1007/s10948-015-3058-x (in press).
[18] S. Chillal, M. Thede, F.J. Litterst, S.N. Gvasaliya, T.A. Shaplygina, S.G. Lushnikov, A. Zheludev, Microscopic coexistence of antiferromagnetic and spin-glass states, Phys. Rev. B 87 (2013) 220403(1)–220403(5).
[19] D.N. Astrov, B.I. Alshin, R.V. Zorin, L.A. Drobyshev, Proc. 11th International Conference on Low Temperature Physics (1968), edited by J. F. Allen, Vol. 2 (1969) 1368.
[20] D.N. Astrov, B.I. Alshin, R.V. Zorin, L.A. Drobyshev, Spontaneous magnetoelectric effect, Sov. Phys. – JETP 55 (1968) 2122–2127.

Please cite this article as: S. Matteppanavar, et al., Origin of room temperature weak-ferromagnetism in antiferromagnetic $Pb(Fe_{2/3}W_{1/3})O_3$ ceramic, Ceramics International (2015), http://dx.doi.org/10.1016/j.ceramint.2015.05.131

[21] W. Brixel, J.P. Rivera, A. Steiner, H. Schmid, Magnetic field induced magnetoelectric effects, (ME)H, in the perovskites Pb_2CoWO_6 and Pb_2FeTaO_6, Ferroelectrics 79 (1988) 201–204.

[22] S.V. Kiselev, R.P. Ozerov, Sov. Phys. Solid State 11 (1969) 1133.

[23] S. Nomura, H. Takabayashi, T. Nakagawa, Dielectric and Magnetic Properties of $Pb(Fe_{1/2}Ta_{1/2})O_3$, Jpn. J. Appl. Phys. **7** (1968) 600.

[24] I.P. Raevskii, D.A. Sarychev, S.A. Bryugeman, L.A. Reznichenko, L.A. Shilkina, O.N. Razumovskaya, V.S. Nikolaev, N.P. Vyshatko, A.N. Salak, Study of cation ordering and magnetic phase transitions in ternary fe-containing perovskite oxides by mössbauer spectroscopy, Crystallogr. Rep. 47 (6) (2002) 1012–1015 (Translated from Kristallografiya, Vol. 47, No. 6, (2002),1081–1084).

[25] Y.u.N. Venevtsev, V.V. SklyarevskiĬ, I.I. Lukashevich, Kristallografiya 21 (5) (1976) 971 (Sov. Phys. Crystallogr. 21, (1976) 556).

[26] G.A. SmolenskiĬ, V.A. Bokov, V.A. Isupov, N.N. Krainik, R.E. Pasynkov, A.I. Sokolov, and N.K. Yushin, The Physics of Ferroelectric Phenomena, Nauka, Leningrad, 1985.

[27] Y.N. Venevtsev, V.V. Gagulin, and V.N. Lyubimov, Magnetoelectrics, Nauka, Moscow, 1982.

Please cite this article as: S. Matteppanavar, et al., Origin of room temperature weak-ferromagnetism in antiferromagnetic $Pb(Fe_{2/3}W_{1/3})O_3$ ceramic, Ceramics International (2015), http://dx.doi.org/10.1016/j.ceramint.2015.05.131